



Particle and gaseous emissions from individual diesel and CNG buses

Å. M. Hallquist¹, M. Jerksjö¹, H. Fallgren¹, J. Westerlund², and Å. Sjödin¹

¹IVL Swedish Environmental Research Institute, Gothenburg, Sweden

²University of Gothenburg, Department of Chemistry and Molecular Biology, Atmospheric Science, Gothenburg, Sweden

Correspondence to: Å. M. Hallquist (asa.hallquist@ivl.se)

Received: 14 July 2012 – Published in Atmos. Chem. Phys. Discuss.: 22 October 2012

Revised: 17 March 2013 – Accepted: 20 March 2013 – Published: 27 May 2013

Abstract. In this study size-resolved particle and gaseous emissions from 28 individual diesel-fuelled and 7 compressed natural gas (CNG)-fuelled buses, selected from an in-use bus fleet, were characterised for real-world dilution scenarios. The method used was based on using CO₂ as a tracer of exhaust gas dilution. The particles were sampled by using an extractive sampling method and analysed with high time resolution instrumentation EEPS (10 Hz) and CO₂ with a non-dispersive infrared gas analyser (LI-840, LI-COR Inc. 1 Hz). The gaseous constituents (CO, HC and NO) were measured by using a remote sensing device (AccuScan RSD 3000, Environmental System Products Inc.). Nitrogen oxides, NO_x, were estimated from NO by using default NO₂/NO_x ratios from the road vehicle emission model HBEFA3.1. The buses studied were diesel-fuelled Euro III–V and CNG-fuelled Enhanced Environmentally Friendly Vehicles (EEVs) with different after-treatment, including selective catalytic reduction (SCR), exhaust gas recirculation (EGR) and with and without diesel particulate filter (DPF). The primary driving mode applied in this study was accelerating mode. However, regarding the particle emissions also a constant speed mode was analysed. The investigated CNG buses emitted on average a higher number of particles but less mass compared to the diesel-fuelled buses. Emission factors for number of particles (EF_{PN}) were EF_{PN, DPF} = 4.4 ± 3.5 × 10¹⁴, EF_{PN, no DPF} = 2.1 ± 1.0 × 10¹⁵ and EF_{PN, CNG} = 7.8 ± 5.7 × 10¹⁵ kg fuel⁻¹. In the accelerating mode, size-resolved emission factors (EFs) showed unimodal number size distributions with peak diameters of 70–90 nm and 10 nm for diesel and CNG buses, respectively. For the constant speed mode, bimodal average number size distributions were obtained for the diesel buses with peak modes of ~10 nm and ~60 nm.

Emission factors for NO_x expressed as NO₂ equivalents for the diesel buses were on average 27 ± 7 g (kg fuel)⁻¹ and for the CNG buses 41 ± 26 g (kg fuel)⁻¹. An anti-relationship between EF_{NO_x} and EF_{PM} was observed especially for buses with no DPF, and there was a positive relationship between EF_{PM} and EF_{CO}.

1 Introduction

It is acknowledged that combustion processes, especially traffic-related emissions, contribute significantly to total particulate air and gaseous pollutants in urban environments. Many epidemiological studies have shown that particles have adverse health effects (Pope and Dockery, 2006). Particles also have an effect on climate either directly via scattering and absorption of radiation or indirectly via its influence on the formation of clouds.

When measuring particle emissions, mass basis is often used. This implies that such data are dominated by large particles. Numerically vehicle exhaust is dominated by ultra-fine particles (UFPs), i.e. particles with a diameter < 100 nm (Janhall et al., 2004; Harrison et al., 1999; Kumar et al., 2010). Therefore an alternative way of presenting particle emissions is needed – i.e. looking at the number of particles emitted – to enable accounting for the small particles that on a mass basis are negligible. Further, health risks are probably dominated by the UFPs (Donaldson et al., 1998; Delfino et al., 2005; Valavanidis et al., 2008). Thus, there is an obvious need to ascertain the emission of particles from traffic regarding number and size in order to establish effective air quality management strategies.

Particles measured in close vicinity of the emission source are primary, i.e. emitted as particles from the tailpipe, or secondary, i.e. formed during the expansion and cooling of the hot exhaust gases. The former are often in the form of agglomerates of solid phase material, whereas the latter are more volatile (Morawska et al., 2008). Additionally, traffic contributes to the formation of secondary organic aerosols (SOAs); however, the magnitude of this contribution is very uncertain (Robinson et al., 2007). This is a chemically induced particle formation (time scales of hours to days) which is very important on a regional and global scale (Hallquist et al., 2009).

The particle emissions from any combustion source can be derived from the emission ratio of the particle concentration to a co-emitted trace gas, such as CO₂ or NO_x (Janhall and Hallquist, 2005). Knowing the emission factor for the chosen trace gas (EF_{gas}), an emission factor for particle number (EF_{PN}) or mass (EF_{PM}) can be estimated (Hak et al., 2009).

$$EF_{PN/PM} = \frac{\Delta_{part}}{\Delta_{gas}} \times EF_{gas}, \quad (1)$$

where Δ_{part} and Δ_{gas} are measured changes in the concentration of particle number/mass and trace gas, respectively. Alternative ways of measuring particle emissions from vehicles are at the kerbside, often giving values for the average fleet, or by chassis dynamometer, measuring vehicles individually (e.g. Janhall et al., 2004; Wang et al., 1997; Ban-Weiss et al., 2010). However, in the latter case it is difficult, if not impossible, to accurately mimic the real-world dilution. Additionally, there are chase-car experiments where the test vehicle is followed by an instrumented vehicle (e.g. Pirjola et al., 2004; Vogt et al., 2003). A challenge with this method is to avoid being influenced by other vehicles as well as keeping the distance between the target vehicle and the chasing vehicle constant. Knowledge about emissions from the on-road fleet under real-world conditions is crucial. In a recent study, EF_{PN} was measured at the kerbside for individual vehicles for real-world dilution (Hak et al., 2009).

Along with particles, nitrogen oxides, NO_x, are depicted as being the most problematic pollutant from internal combustion engines (Lopez et al., 2009). In order to meet the lower NO_x and particle emission levels introduced for heavy duty vehicles (HDVs), exhaust gas after-treatment has become necessary. To reduce particle emissions from HDVs, diesel particulate filters (DPFs) are widely used. An example of after-treatment technology to reduce NO_x is selective catalytic reduction (SCR), which can be found in power plants, ships and lately also in HDVs. The most common method is SCR with urea injection due to urea's low toxicity and ease in handling, but direct injection of NH₃ can also be used. In the SCR system the urea/water mixture (e.g. AdBlue®) is first added to the exhaust gas which becomes hydrolysed to NH₃ and CO₂. In the SCR catalyst section NH₃ reacts with NO_x to form N₂ and H₂O. Another common approach to reduce NO_x emissions is exhaust gas recirculation (EGR). By keep-

ing a low combustion temperature and low oxygen content the formation of NO_x is unfavourable; this can be achieved by recirculating a small fraction of the exhaust gas back to the cylinders.

Emissions from new HDVs in Europe are regulated by Euro standards. Currently in force since 2008 is the Euro V standard, and the Euro VI standard will be implemented in 2013. Enhanced Environmentally Friendly Vehicle, EEV, is a voluntary environmental standard which requires lower emission levels than Euro V. It was introduced together with the Euro IV and Euro V emission standards as an incentive to develop vehicles with even lower emission levels than required by regulations, and is mostly applicable to CNG heavy duty vehicles.

In order to meet the challenges with increased transportation, decreased oil resources and enhanced greenhouse gas emissions, the European Union has decided on a 10% substitution of traditional fuels in the road transport sector (petrol and conventional diesel) by alternative fuels by the year 2020. However, the emissions from vehicles using alternative fuels have to be thoroughly studied to avoid introduction of air pollutants that can have severe health/environmental effects or other so far unknown effects or, alternatively, to establish the advantages from using these fuels.

In the literature there are some studies that have compared the particle emissions from diesel-fuelled and CNG-fuelled buses (Jayaratne et al., 2008, 2009; Wang et al., 1997; Ullman et al., 2003; Lanni et al., 2003; Norman et al., 2002; Clark et al., 1999). This study takes these investigations further by determining both gaseous (NO_x, CO and HC) and size-resolved particle emission factors for CNG and diesel buses belonging to different Euro classes with various after-treatment equipment, i.e. EGR and SCR, for real-world dilution scenarios.

2 Experimental method

In this study particle and gaseous emissions from individual vehicles were determined by measuring the concentration change in the diluted exhaust plume compared to the concentrations before the passage and relative to the change in CO₂ concentration. By this method it is not necessary to measure absolute concentrations as the relation to CO₂ is assumed to be constant during dilution (Jayaratne et al., 2005, 2010; Canagaratna et al., 2004; Shi et al., 2002; Hak et al., 2009). In addition, this method enables deriving size-resolved EFs (Janhall and Hallquist, 2005).

In total 35 different buses were studied, 28 diesel buses and 7 CNG buses. A summary of their technical characteristics including fuel used, Euro class, after-treatment system, year taken into service and kilometres travelled is shown in Table 1.

The measurements were performed at five different locations in connection to the bus depots with limited influence

Table 1. Technical data of the buses studied.

Bus no	Euro class	Fuel ^a	After-treatment ^b	Year taken into service	Distance travelled (10 ³ km)
1	III ^c	Diesel	SCR, DPF	2004	525
2	III ^c	Diesel	SCR, DPF	2004	516
3	III	Diesel	DPF	2003	454
4	III	Diesel	DPF	2002	995
5	III	Diesel	DPF	2002	584
6	III	Diesel	DPF	2002	523
7	III	Diesel	–	2004	232
8	III	Diesel	–	2004	285
9	IV	Diesel	EGR, DPF	2006	393
10	IV	Diesel	EGR, DPF	2006	3.74
11	IV	Diesel	EGR	2008	116
12	IV	Diesel	EGR	2006	597
13	IV	Diesel	EGR	2010	182
14	EEV ^d	CNG	–	1999	598
15	EEV	CNG	–	2004	397
16	EEV	CNG	–	2004	365
17	EEV	CNG	–	2008	157
18	EEV	CNG	–	2008	153
19	EEV	CNG	EGR	2004	450
20	EEV	CNG	EGR	2004	482
21	V	Diesel	SCR, DPF	2009	55.8
22	V	Diesel	SCR	2009	n.a. ^e
23	V	Diesel	SCR	2007	347
24	V	Diesel	SCR	2007	307
25	V	Diesel	SCR	2009	171
26	V	Diesel	SCR	2007	336
27	V	Diesel	SCR	2007	351
28	V	Diesel	SCR	2007	143
29	V	Diesel	EGR, DPF	2009	123
30	V	Diesel	SCR	2007	28.6
31	V	Diesel	SCR	2007	3924
32	V	Diesel	SCR	2007	209
33	V	Diesel	SCR	2007	371
34	V	Diesel	SCR	2009	104
35	V	Diesel	SCR	2010	71.2

^a Diesel = MK1 < 10 ppm S

^b SCR=selective catalytic reduction, EGR=exhaust gas recirculation, DPF=diesel particulate filter

^c Modified Euro III, now classified as Euro V

^d EEV=Enhanced Environmentally Friendly Vehicle

^e n.a.=not available.

from other traffic. Each bus passed the remote sensing and EEPS instrumentation in two driving modes: (1) acceleration from standstill to about 20 km h⁻¹, and (2) constant speed of about 20 km h⁻¹. Before the buses were measured they were driven a distance, assuring the engines to be fully warmed up. Each bus was tested at least three times, but often more repetitions were performed.

2.1 Particle sampling

The sampling of the particle emissions was conducted according to Hak et al. (2009), i.e. an extractive sampling of the passing bus plumes where the sample was continuously

drawn through a cord-reinforced flexible conductive tubing. The particles were measured with an EEPS (Engine Exhaust Particle Sizer Spectrometer, Model 3090, TSI Inc.). With this instrument, particle size distributions both regarding mass and number can be obtained in the size range of 5.6–560 nm and with a time resolution of 10 Hz. When determining the mass of particles emitted, spherical particles with unit density were assumed. The CO₂ concentration was measured with a non-dispersive infrared gas analyser (LI-840, LI-COR Inc.) with a time resolution of 1 Hz (Fig. 1).

In order to prevent the influence of the ambient temperature on the measurements for the different measurement

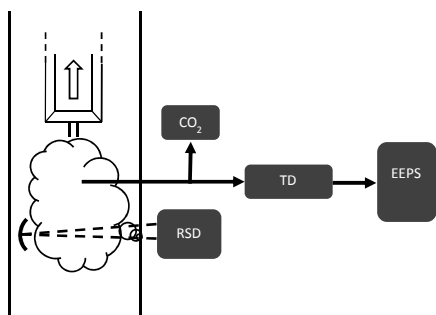


Fig. 1. Schematic of the experimental set-up used. EEPS (Engine Exhaust Particle Sizer Spectrometer, Model 3090, TSI Inc.), RSD (Remote Sensing Device, AccuScan RSD 3000, Environmental System Products Inc.) and TD (thermodenuder; Dekati).

days, the extracted sample flow was heated to 298 K before the analysis using a thermodenuder (TD; Dekati). Size-dependent aerosol losses within the TD were accounted for (user manual).

2.2 Gas sampling

The gaseous constituents NO, HC and CO were measured by using a remote sensing device (AccuScan RSD 3000, Environmental System Products Inc.). This equipment was set up with a transmitter and a receiver on one side of the passing lane and a reflector on the other (Fig. 1). The principle of this instrument has been described in detail elsewhere (Burgard et al., 2006) and will only be briefly presented here. This instrumental set-up generates and monitors a co-linear beam of IR and UV light emitted and reflected. Concentrations are determined relative to the concentration of CO₂ with a time resolution of 100 Hz. For detecting CO, HC and CO₂ the absorptions in the IR region at 2150 cm⁻¹, 2970 cm⁻¹ and 2350 cm⁻¹, respectively, are used. For NO the absorption in the UV region at 227 nm is used. The instrumental noise of the used RSD 3000 unit was estimated with the method described in Burgard et al. (2006) using a dataset from an earlier remote sensing study, comprising more than 20 000 on-road emission measurements on passenger cars. The detection limits were then estimated as three times the standard deviation of the noise and were determined to be 18 g (kg fuel)⁻¹, 14 g (kg fuel)⁻¹ and 5 g (kg fuel)⁻¹ for CO, HC and NO, respectively.

Calibrations were conducted every 1.5–2 h of measurements by using a certified gas mixture containing 1510 ppm propane, 1580 ppm NO, 1600 ppm NO_x, 3.00 % CO and 12.8 % CO₂ in N₂ (AGA Gas). The gaseous data was retrieved from the RSD system as ppm or %.

2.3 Calculation of emission factors (EFs)

Particle emission factors were derived by assuming the CO₂ concentration to be directly proportional to the fuel consump-

tion, hence assuming complete combustion. For the gaseous constituents also the measured HC and CO were accounted for. In the calculations a carbon fraction of 0.865 and 0.749 for diesel and CNG fuel, respectively, was used. In this study the emission factors are presented as mass or number per kg fuel used. The gaseous pollutant emission factor for each compound (CO, HC or NO) per kilogram of fuel burnt was for diesel-fuelled vehicles calculated by applying Eq. (2) (Burgard et al., 2006) and for CNG-fuelled vehicles by applying Eq. (3):

$$EF_{\text{gas}} = \frac{CF_{\text{Fuel}} \times SF \times M_{\text{gas}}}{M_{\text{C}}} \times \frac{\frac{\text{gas}}{\text{CO}_2}}{\left(1 + \frac{\text{CO}}{\text{CO}_2} + 6 \frac{\text{HC}}{\text{CO}_2}\right)}, \quad (2)$$

$$EF_{\text{gas}} = \frac{CF_{\text{Fuel}} \times SF \times M_{\text{gas}}}{M_{\text{C}}} \times \frac{\frac{\text{gas}}{\text{CO}_2}}{\left(1 + \frac{\text{CO}}{\text{CO}_2} + 4.3 \frac{\text{HC}}{\text{CO}_2}\right)}, \quad (3)$$

where CF_{Fuel} is the carbon mass fraction of the fuels, M_{gas} and M_{C} are the molar mass of CO, HC, NO and C, respectively, and SF is a scaling factor. The RSD unit is calibrated with propane, and the hydrocarbons in the exhaust gas from diesel vehicles are assumed to be similar to the calibration gas, hence the molar mass of propane was used as M_{HC} in Eq. (2). In Eq. (3) the molar mass of methane was used as this is the major constituent of CNG. The scaling factor is only applicable for determining HC; for all the other gaseous compounds SF is equal to 1. An SF is used to compensate for the known difference between non-dispersive infrared (NDIR)-based measurements and flame ionization detector (FID)-based measurements, a factor of 2 for diesel-fuelled vehicles (Singer et al., 1998) and a factor of 4.3 for CNG-fuelled vehicles (Stephens et al., 1996; Singer et al., 1998). The factor of 6 in Eq. (2) arises from the carbon atoms per molecule of propane multiplied with the scaling factor of 2.

Since the remote sensing device measures NO and not NO₂, the reported NO_x emission factors have been estimated from measured NO and the default NO₂/NO_x ratios from the HBEFA 3.1 road vehicle emission model (HBEFA3.1, 2010); see Table 2. The NO_x emission factors were calculated by using Eq. (4):

$$EF_{\text{NO}_x} = \frac{EF_{\text{NO}}}{1 - \left(\frac{\text{NO}_2}{\text{NO}_x}\right)}, \quad (4)$$

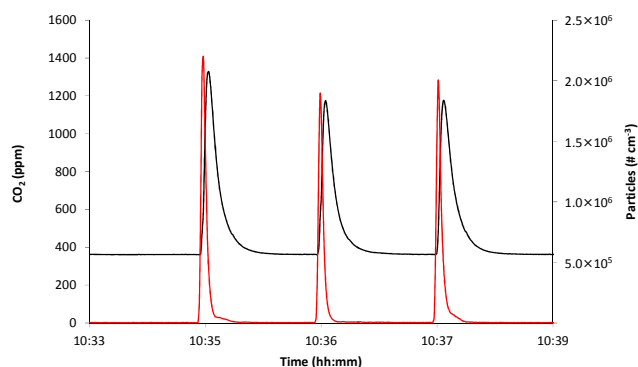
where EF_{NO} is expressed as grams of equivalent NO₂ per kg fuel. Reporting NO_x emissions as equivalent NO₂ complies with HDV emission standards (Shorter et al., 2005).

In order to be able to compare with studies expressing EFs in mass/number per km, the EFs in this study were re-calculated by using the average fuel consumption reported for the tested diesel and CNG buses, 0.38 L km⁻¹ and 0.735 Nm³ km⁻¹, respectively. For the calculations a density of 0.815 kg dm⁻³ and 0.70 kg m⁻³ was assumed (Swedish Environmental Protection Agency, 2013). These EFs (in

Table 2. HBEFA 3.1 Emission factors, fuel consumption (FC) and NO₂ to NO_x ratios for Ubus Std > 15–18 t Urban Access Road/30/Stop + Go.

	EF _{PN} 10 ¹⁴ (kg fuel) ⁻¹	EF _{PM} g (kg fuel) ⁻¹	EF _{NO_x} g (kg fuel) ⁻¹	FC g km ⁻¹	NO ₂ /NO _x %
Euro III	8.3	0.70	37	444	7
Euro III <i>DPF</i>	1.6	0.18	37	448	30
Euro IV <i>EGR</i>	4.1	0.18	23	357	21
Euro IV <i>EGR, DPF</i>	0.69	0.012	23	365	25
Euro V <i>EGR, DPF</i>	0.68	0.012	14	372	25
Euro V <i>SCR</i>	2.0	0.20	38	353	7
Euro V <i>SCR, DPF</i>	0.20	0.0078	37	360	25*
CNG EEV	0.072	0.17	44	510	25

* This NO₂/NO_x ratio has also been used in this study for Euro III buses with SCR and DPF.


Fig. 2. Example of emission signals from three successive individual passages of the same bus in *accelerating mode*. Particle number (red line) and CO₂ concentration (black line).

number/mass km⁻¹) will be a lower limit as the fuel consumption during acceleration is expected to be higher.

2.4 Modelling

The measured EFs (both particles and gaseous) were also compared to modelled EFs by using the HBEFA 3.1 (2010). This model provides EFs in g km⁻¹ for six main categories of road vehicles: passenger cars, light duty vehicles, heavy goods vehicles, urban buses, coaches and motorcycles (including mopeds). These main categories are further divided into size classes, type of fuel and emission standards. For all Euro IV and Euro V HDVs the model provides EFs separately for vehicles with SCR and for vehicles with EGR. For the class *urban buses* EFs are also provided for vehicles both with and without DPF. Furthermore, the emission factors are given for a large number of traffic situations based on emis-

sion measurements according to different sets of real-world driving cycles (HBEFA3.1, 2010).

The measured EFs in this work were compared to modelled data for a standard urban bus (15–18 tons). The driving pattern was classified according to the HBEFA 3.1 traffic situation scheme as *urban access road* with a posted speed of 30 km h⁻¹ and with stop-and-go traffic. The stop-and-go traffic flow is defined as a driving cycle including many accelerations from standstill which was considered to be the driving pattern that best described the driving pattern used in the present measurements for the accelerating mode. All EFs were recalculated from g km⁻¹ to g kg⁻¹ by using the specific fuel consumption given in HBEFA 3.1. Used emission factors, fuel consumption and NO₂ to NO_x ratios are presented in Table 2.

3 Results and discussion

3.1 Emission signal

An example of typical signals in number of particles and CO₂ concentration during a bus passage is shown in Fig. 2. In this figure three successive bus passages for the same vehicle are displayed for the accelerating mode. The shape of the CO₂ peak is broader than the particle peak, which is due to the use of a small volume before the CO₂ analyser, extending the time available for the instrument to process the gas sample in order to prevent concentration peaks out of the instrument's measurement range. In Table 3 the measurement results for all the tested buses are presented. Generally there is higher variation in the data for the constant speed mode tests compared to the accelerating mode tests, which is primarily due to difficulties for the drivers to keep the same

Table 3. EF for particle number (EF_{PN}), mass (EF_{PM}) and gaseous compounds for all the buses studied in accelerating mode (acc) and constant speed mode (const). Stated errors are at the statistical 95 % confidence interval.

Bus no	Euro class	EF _{PN, acc} # (kg fuel) ⁻¹ 10 ¹⁴	EF _{PN, const} # (kg fuel) ⁻¹ 10 ¹⁴	EF _{PM, acc} mg (kg fuel) ⁻¹	EF _{PM, const} mg (kg fuel) ⁻¹	EF _{CO, acc} g (kg fuel) ⁻¹	EF _{NO_x, acc} ^a g (kg fuel) ⁻¹
1	III ^b	1.9 ± 0.2	1.1 ± 0.2	62 ± 11	41 ± 12	< 18	22 ± 3
2	III ^b	23 ± 1 ^c	9.7 ± 0.5	2465 ± 1352 ^c	142 ± 23	52 ± 10	28 ± 3
3	III	0.46 ± 0.34	4.2 ± 2.6	31 ± 19	273 ± 161	< 18	24 ± 16
4	III	n.a ^d	3.4 ± 1.0	171 ± 126	151 ± 41	< 18	30 ± 5
5	III	0.11 ± 0.01	0.12 ± 0.04	6.7 ± 3.1	n.a	< 18	< 5 ^e
6	III	11 ± 2	n.a	681 ± 236	n.a	< 18	19 ± 2
7	III	33 ± 6	n.a	1566 ± 419	n.a	25 ± 14	22 ± 7
8	III	45 ± 13	n.a	2074 ± 619	n.a	36 ± 17	< 5
9	IV	13 ± 0.1	3.1 ± 0.5	650 ± 45	61 ± 12	< 18	< 5
10	IV	5.1 ± 0.6	2.6 ± 0.7	177 ± 23	58 ± 8	< 18	20 ± 2
11	IV	39 ± 23	47 ± 42	1883 ± 908	489	< 18	9 ± 3
12	IV	44 ± 7	n.a	3089 ± 818	n.a	52 ± 35	< 5
13	IV	13 ± 8	5.8 ± 1.8	562 ± 469	91 ± 34	< 18	19 ± 5
14	EEV	173 ± 25	n.a	36 ± 25	n.a	< 18	9 ± 3
15	EEV	45 ± 41	n.a	15 ± 9	n.a	< 18	43 ± 21
16	EEV	1.4 ± 1.0	n.a	3.5 ± 1.6	n.a	< 18	59 ± 9
17	EEV	155 ± 33	n.a	60 ± 15	n.a	< 18	77 ± 4
18	EEV	144 ± 12	n.a	49 ± 24	n.a	< 18	89 ± 27
19	EEV	11 ± 7	5.6 ± 9.4	3.0 ± 1.4	1.9 ± 0.5	< 18	< 5
20	EEV	13 ± 4	20 ± 7	0.38 ± 0.22	n.a	< 18	< 5
21	V	2.9 ± 0.5	2.4 ± 0.5	76 ± 14	46 ± 12	< 18	63 ± 5
22	V	4.4 ± 1.5	2.7 ± 0.5	125 ± 52	47 ± 13	< 18	45 ± 5
23	V	8.4 ± 0.9	5.2 ± 1.7	175 ± 36	63 ± 23	< 18	50 ± 2
24	V	11 ± 1	20 ± 4	184 ± 14	204 ± 109	< 18	38 ± 6
25	V	12 ± 1	7.4 ± 3.3	242 ± 26	56 ± 26	< 18	27 ± 12
26	V	11 ± 1	12 ± 5	181 ± 11	205 ± 147	< 18	49 ± 0
27	V	8.3 ± 1.4	4.1 ± 0.7	178 ± 42	61 ± 15	< 18	42 ± 27
28	V	15 ± 6	3.2 ± 0.6	318 ± 167	41 ± 8	< 18	29 ± 11
29	V	0.36 ± 0.45	0.095 ± 0.028	3.8 ± 2.8	4.9 ± 5.2	< 18	< 5
30	V	5.8 ± 0.5	5.0 ± 0.3	298 ± 25	77 ± 19	19 ± 21	58 ± 4
31	V	7.6 ± 2.9	33 ± 16	240 ± 87	509 ± 264	28 ± 9	43 ± 4
32	V	15 ± 6	3.9 ± 2.7	766 ± 429	398 ± 260	< 18	20 ± 2
33	V	7.2 ± 0.9	n.a	232 ± 77	n.a	< 18	51 ± 6
34	V	92 ± 42	n.a	165 ± 66	n.a	< 18	17 ± 20
35	V	5.0 ± 2.0	15 ± 5	246 ± 128	385 ± 275	< 18	15 ± 11

^a In NO₂ equivalents^b Modified Euro III, now classified as Euro V^c Omitted when calculating average size distributions and total numbers^d n.a = not available^e Less than 8 g (kg fuel)⁻¹ NO as NO₂ equivalents.

constant speed/rpm while passing the measurement equipment on repeated occasions. However, vehicles identified as high-emitters in the accelerating mode were also generally identified as high-emitters in the constant speed mode (Table 3).

3.2 EF_{part} for different Euro classes

In Fig. 3 the derived EF_{PN} and EF_{PM} for each Euro class are shown for the *accelerating mode*. Generally, higher EFs were

obtained for buses without DPFs regarding both number and mass of particles emitted. The CNG buses emitted on average a higher number of particles compared to the diesel-fuelled buses, which is in line with previous studies (Jayaratne et al., 2008, 2010). When comparing the average EF_{PN} of the investigated diesel-fuelled buses with the CNG-fuelled buses for the *accelerating mode*, the EF_{PN} for CNG buses were about five times higher ($1.6 \pm 0.7 \times 10^{15}$ vs. $7.8 \pm 5.7 \times 10^{15}$ (kg fuel)⁻¹), which is similar to results obtained by Jayaratne et al. (2008) (4.0×10^{15} vs. 2.1×10^{16} (kg fuel)⁻¹), when

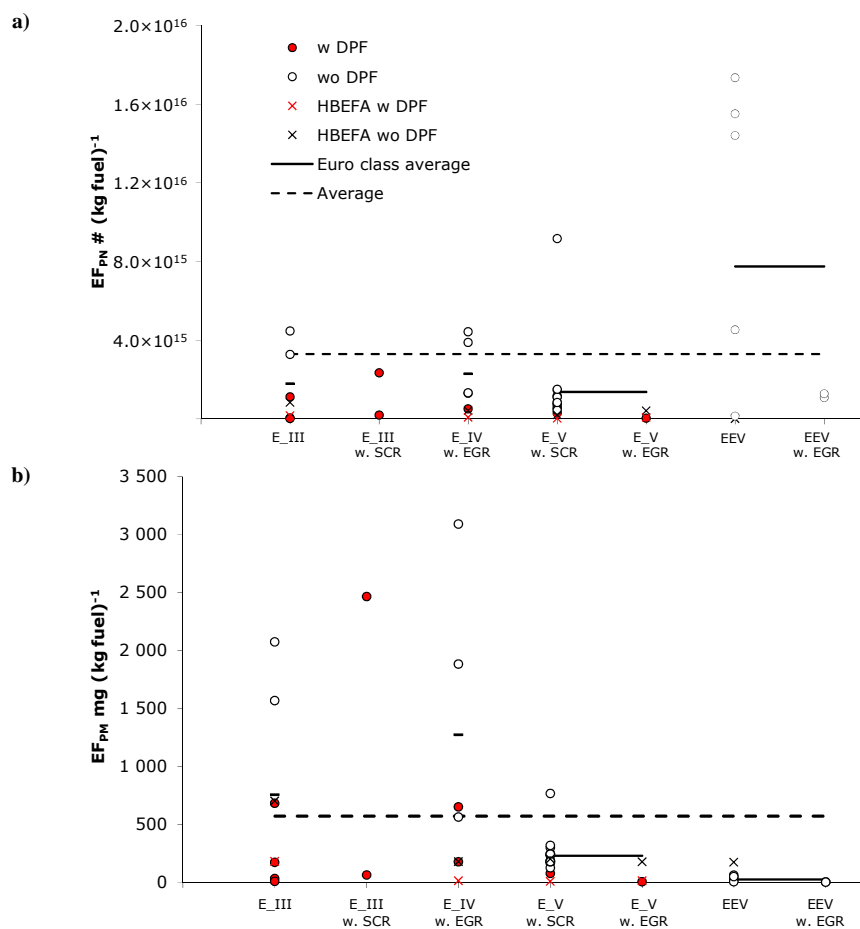


Fig. 3. EF_{PN} (a) and EF_{PM} (b) for all the buses studied divided into Euro class for the driving mode *acceleration*. Without DPF (white circles), with DPF (red circles), average of all represented Euro classes (dashed line), average of an individual represented Euro class (solid line). Crosses are EFs obtained by the HBEFA 3.1 model with DPF (red) and without (black).

using the same fuel C-content assumption as in this study. However, in the case of mass of particles, the emissions from the CNG buses were on average lower compared to diesel buses.

Figure 3 also shows that a diesel bus with DPF for the *accelerating mode* emits on average 5 times less than a diesel bus without DPF regarding number of particles and 3 times less regarding mass of particles ($4.4 \pm 3.5 \times 10^{14}$ vs. $2.1 \pm 1.0 \times 10^{15} \text{ kg}^{-1}$ and 206 ± 175 vs. $696 \pm 398 \text{ mg kg}^{-1}$).

Regarding number of particles, only buses without DPF were having EFs above the average EF of all tested vehicles (see Fig. 3). The largest scatter in EF_{PN} was, however, obtained for the CNG-fuelled buses. Out of the 15 highest PN-emitting buses, there were five gas buses (in total 7 CNG buses were tested) and 13 had no DPF installed. Regarding mass of particles, vehicles emitting above the average EF_{PM} of all tested buses belonged to all Euro classes, except for buses representing Euro V with EGR and the CNG-fuelled buses. The 15 highest PM-emitting buses were only

diesel-fuelled buses; 12 had no DPF and four of the total five tested Euro IV with EGR buses were among these vehicles. The higher masses obtained for EGR-equipped buses without DPF may be due to the decrease in oxygen content when some of the exhaust gas is re-circulated, which favours soot formation (Seinfeld and Pandis, 1998; Maricq, 2007).

For comparison, modelled values of EF_{PN} and EF_{PM} using the HBFA 3.1 model are shown in Table 2. The modelled values are generally significantly lower than the measured values. A possible explanation for this can be different driving modes, acceleration versus route, including start and stops but also constant speed mode. As indicated by Table 3, $EF_{PN/PM}$ was generally lower for constant speed mode compared to acceleration. Modelled EF_{PN} was the lowest for CNG buses and highest for diesel buses, whereas the opposite was found in this study. A reason for this can be that the particle number emissions that the HBEFA model is based on often follow the PMP protocol, involving heating the particle sample to 300 °C, and the CNG particles are suggested to be volatile (Jayaratne et al., 2012).

For the *constant speed mode* higher EFs were also generally obtained for buses without DPF. However, too few CNG buses were analysed in this driving mode to make a comparison between EFs for CNG buses and diesel buses.

Table 4 is a summary of the average EF_{PN} and EF_{PM} for diesel buses with and without DPF and for CNG buses obtained in this study (recalculated to km^{-1}) and a comparison to other studies. Generally, the average EFs obtained for number of particles are within the reported ranges for diesel buses but somewhat higher for the CNG-fuelled buses. The average EF_{PM} measured for diesel buses in this study are also within the ranges reported in other studies. In Table 4 most EF_{PM} data is for larger particle size ranges. However, as most particles related to road traffic combustion are below 560 nm, as is shown in Figs. 4 and 5, the particle size range used in this study is comparable to PM_{10} and $PM_{2.5}$. However, important to note is that road measurements of PM_{10} and $PM_{2.5}$ can include non-combustion-related particle emissions, e.g. re-suspension, and can hence be higher. It is a large variation in the reported data regarding the mass emitted for CNG buses and the data reported in this study are similar to results by Jayaratne et al. (2009) and Nylund et al. (2004).

In Lopez et al. (2009) a Euro IV diesel-fuelled bus equipped with EGR and DPF and a Euro IV diesel-fuelled bus equipped with SCR were analysed for a full driving cycle for which EF_{PM} were determined to be 49 ± 1 and 73 ± 4 $\text{mg vehicle}^{-1} \text{ km}^{-1}$, respectively. In this study no Euro IV with SCR were studied, but Euro V were studied, and the average EF_{PM} for these buses (when excluding one extreme) was 68 ± 11 $\text{mg vehicle}^{-1} \text{ km}^{-1}$. Two Euro IV diesel-fuelled buses equipped with EGR and DPF were tested: one gave similar EF_{PM} to Lopez et al. (2009), 55 $\text{mg vehicle}^{-1} \text{ km}^{-1}$, and the other significantly higher EF_{PM} , 201 $\text{mg vehicle}^{-1} \text{ km}^{-1}$.

The data presented in this study (Table 3) is a reflection of the true variation in an in-use regional bus fleet, where the variation found between similar buses (e.g. regarding fuel type and after-treatment technology) within the same Euro class can be due to engine specifics, maintenance and malfunction.

3.3 Size-resolved EF, number and mass

In Fig. 4, size-resolved EF_{PN} for each bus class in the *accelerating mode* are shown, i.e. diesel buses with (Fig. 4a) and without (Fig. 4b) DPF and CNG buses (Fig. 4c). All classes show more or less a unimodal number size distribution. Diesel buses emit larger particles compared to CNG buses, peak diameter 70–90 nm and 10 nm, respectively, which is similar to results reported in Jayaratne et al. (2009) (80–90 nm and 10–12 nm, respectively). The lack of larger particles in the emissions from CNG-fuelled buses decreases the available surface area, hence favouring nucleation over adsorption/condensation of supersaturated vapours. This enhanced nucleation is one reason for

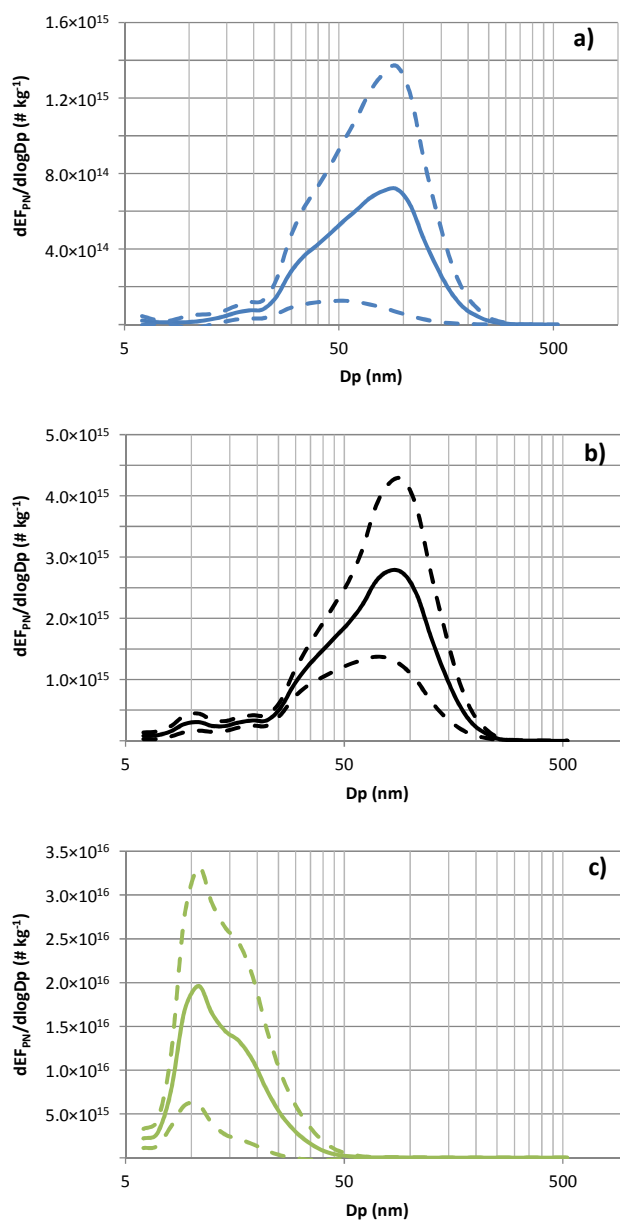


Fig. 4. Size-resolved average EF_{PN} for diesel buses (Euro III–V) with DPF (a) and without DPF (b) and for CNG buses (c) for the driving mode *acceleration*. Solid lines represent averages and dashed lines the statistical 95 % confidence interval. For the data presented in graph (b) one bus (no. 34) was excluded showing much higher size-resolved EF_{PN} and with a peak size of ~ 17 nm.

the larger average particle number emissions for the tested CNG buses (Kumar et al., 2010). The mass size distribution shows that the diesel engines in the accelerating mode primarily emit particles with a diameter of ~ 150 nm and that CNG buses exhibit on average a bimodal mass size distribution with one mode peaking at about 25 nm and another at ~ 125 nm (Fig. 5).

Table 4. Comparison of emission data for particle number and mass from present study with selected literature data.

PN						
Ref	Dp range nm	Speed km h ⁻¹	Vehicle type	Method	Instrument	EF _{PN} # vehicle ⁻¹ km ⁻¹ 10 ¹⁴
This study	5.6–560	acc.	bus diesel	road	EEPS	1.4 ± 1.1 ^a
	5.6–560	acc.	bus diesel	road	EEPS	6.5 ± 3.2 ^b
	5.6–560	acc.	bus CNG	road	EEPS	40 ± 29
Beddows and Harrison (2008)	> 7		HDV	aggregated	CPC	7.06
Birmili et al. (2009)	10–500	75–90	HDV	CFD	TDMPS	29.6 ± 3.5
Corsmeier et al. (2005)	30–300	85	HDV	box model		7.8
Jayaratne et al. (2010)	> 5	80	bus diesel	dynamometer	CPC	1.71
Jayaratne et al. (2010)	> 5	80	bus CNG	dynamometer	CPC	5.4
Jayaratne et al. (2009)	5–160	25–100 % ^c	bus diesel	dynamometer	SMPS	1.2–18
Jayaratne et al. (2009)	5–160	25–100 % ^c	bus CNG	dynamometer	SMPS	1.0–14
Jones and Harrison (2006)	11–450	< 50	HDV	street canyon	SMPS	6.36
Keogh et al. (2010)	ns ^d		HDV	statistical ^e	CPC	65 (60.19–69.81)
Keogh et al. (2010)	ns		HDV	statistical ^e	SMPS	3.08
Morawska et al. (2008)	10–30		HDV	review		2.14–37.8
Morawska et al. (2008)	18–50		HDV	review		1.55–8.2
Morawska et al. (2008)	18–100		HDV	review		1.7–10.5
Morawska et al. (2008)	30–100		HDV	review		3.19
Wang et al. (2010)	10–700	90–110	HDV	road	DMPS	17.5
Wang et al. (2010)	10–700	0–50	HDV	road	DMPS	22.1
Keogh et al. (2010)	ns		LDV	statistical ^e	CPC	3.63
PM						
Ref	PM(x)	Speed km h ⁻¹	Vehicle type	Method	Instruments	EF _{PM} mg vehicle ⁻¹ km ⁻¹
This study	5.6–560	acc.	bus diesel	road	EEPS	64 ± 54 ^a
	5.6–560	acc.	bus diesel	road	EEPS	215 ± 123 ^b
	5.6–560	acc.	bus CNG	road	EEPS	12 ± 9
Clark et al. (1999)	PM	d.c	bus diesel	dynamometer	ns	190–1450
Clark et al. (1999)	PM	d.c	bus CNG	dynamometer	ns	4–100
Jayaratne et al. (2009)	PM ₁₀	25–100 % ^c	bus diesel	dynamometer	DustTrak	46.5–668.6
Jayaratne et al. (2009)	PM ₁₀	25–100 % ^c	bus CNG	dynamometer	DustTrak	0.01–1.3
Jones and Harrison (2006)	PM ₁₀	< 50	HDV	street canyon	TEOM	370 ± 32
Jones and Harrison (2006)	PM _{2.5}	< 50	HDV	street canyon	TEOM	179 ± 22
Keogh et al. (2010)	PM ₁₀	Ns	HDV	statistical ^e	several	538
Keogh et al. (2010)	PM _{2.5}	Ns	HDV	statistical ^e	several	302 (236–367)
Lanni et al. (2003)	PM	d.c ^f	bus diesel	dynamometer	gravimetric	72
Lanni et al. (2003)	PM	d.c	bus CNG	dynamometer	gravimetric	86
Lopez et al. (2009)	PM	d.c	bus EIV EGR + DPF	on-board	MAHA	49 ± 1 ^g
Lopez et al. (2009)	PM	d.c	bus EIV SCR	on-board	MAHA	73 ± 4 ^g
Nylund et al. (2004)	PM	d.c	bus diesel	dynamometer	ns	20–170
Nylund et al. (2004)	PM	d.c	bus CNG	dynamometer	ns	5–10
Ullman et al. (2003)	PM	d.c	bus diesel	dynamometer	gravimetric	296
Ullman et al. (2003)	PM	d.c	bus CNG	dynamometer	gravimetric	84
Wang et al. (2010)	PM _{2.5}	90–110	HDV	road ^h	TEOM	233 ± 18
Wang et al. (2010)	PM _{2.5}	0–50	HDV	road ⁱ	TEOM	628 ± 50
Wang et al. (2010)	PM ₁₀	90–110	HDV	road ^h	TEOM	1087 ± 68
Wang et al. (1997)	PM	d.c	bus diesel	dynamometer	gravimetric	1960
Wang et al. (1997)	PM	d.c	bus CNG/LNG	dynamometer	gravimetric	48
Keogh et al. (2010)	PM ₁₀	Ns	LDV	statistical ^e	several	153
Keogh et al. (2010)	PM _{2.5}	Ns	LDV	statistical ^e	several	33

^a DPF
^b no DPF
^c % of max engine power
^d ns = not stated
^e based on 667 EFs
^f d.c = driving cycle
^g sd
^h highway
ⁱ urban

Table 5. Comparison of emission data for NO_x, VOC and CO from present study with selected literature data.

Ref	Speed km h ⁻¹	Vehicle type	Method	EF _{NO_x} g km ⁻¹	EF _{VOC} g km ⁻¹	EF _{CO} g km ⁻¹
This study	acc	Euro III	road	5 ± 3	< 4 ^a	5 ± 5
	acc	Euro IV	road	4 ± 2	< 4 ^a	5 ± 5
	acc	Euro V	road	11 ± 3	< 4 ^a	3 ± 1
	acc	CNG bus	road	21 ± 14	< 4 ^a	< 3
Chen et al. (2007)	< 85	HDV	on-board	6.54	1.88	4.96
Clark et al. (1999)	d.c ^b	bus diesel	dynamometer	28.5–37.5	0.1–0.6 ^c	2.5–18.0
Clark et al. (1999)	d.c	bus CNG	dynamometer	10.9–23.8	16.9–32.2 ^c	0.2–13.3
Corsmeier et al. (2005)	85	HDV	on-road	6.86 ± 1.57	–	–
Jayaratne et al. (2009)	25–100 %	bus diesel	dynamometer	6.7–18	–	–
Jayaratne et al. (2009)	25–100 %	bus CNG	dynamometer	5.5–32	–	–
Jones and Harrison (2006)	< 50	HDV	street canyon	5.19	–	–
Kristensson et al. (2004)	75	HDV	tunnel	8.0 ± 0.8	–	–
Lanni et al. (2003)	d.c	bus diesel DPF	dynamometer	38.4	0.1	0.2
Lanni et al. (2003)	d.c	bus CNG	dynamometer	68.9	93.9	76.4
Lopez et al. (2009)	d.c	bus EIV EGR + DPF	on-board	6.925	0.068 ^c	0.250
Lopez et al. (2009)	d.c	bus EIV SCR	on-board	6.121	0.053 ^c	1.716
Nylund et al. (2004)	d.c	bus diesel	dynamometer	8–9	0.05–0.4 ^c	–
Nylund et al. (2004)	d.c	bus CNG	dynamometer	2–7	0.25–2 ^c	–
Ullman et al. (2003)	d.c	bus diesel	dynamometer	22.7	0.6	2.8
Ullman et al. (2003)	d.c	bus CNG	dynamometer	26.1	15.0	7.7
Wang et al. (2010)	90	HDV	on-road	9.8 ± 0.29	–	–
Wang et al. (2010)	0–50	HDV	on-road	11.9 ± 0.59	–	–
Wang et al. (2008)		bus	calculated ^d	18.19	3.71	37.15
Wang et al. (2008)		truck	calculated ^d	9.3	2.99	34.79

^a In this study HC^b d.c = driving cycle^c THC^d calculated from emission inventory

For the analysis of the average size-resolved EF_{PN/PM} for buses without DPF (Figs. 4b and 5b), one bus (no. 34) was excluded showing much higher size-resolved EF_{PN} and with a peak size of ~17 nm. For this bus the average size-resolved EF_{PM} was bimodal with peak sizes of ~30 nm and ~190 nm. The reason for this discrepancy is not known but could be due to maintenance or malfunction of this particular bus.

For the *constant speed mode* the characteristic bimodal number size distributions were obtained for the diesel buses with and without DPF, with one mode peaking at ~10 nm (nucleation mode) and the other at ~60 nm (soot mode/accumulation mode) (Fig. 6) (Maricq, 2007). The reason for the different average number size distributions between accelerating and constant speed mode may be more available surface area in the accelerating mode, hence favouring adsorption/condensation over nucleation. In acceleration from standstill the engine load is close to its maximum, and Jayaratne et al. (2009) also obtained a unimodal number size distribution for a diesel bus at 100 % load.

3.4 Comparison of EF_{part} and EF_{gas} (NO_x, HC and CO)

The highest NO_x values were obtained for the CNG buses compared to all the other Euro classes of diesel buses; however, the scatter was largest for the CNG buses as well (41 ± 26 g kg⁻¹) (Fig. 7), which is in accordance with Ekström et al. (2005). Possible reasons for this variability may be vehicle maintenance and variations in the CNG composition (Shorter et al., 2005; Ayala et al., 2002). The EF for NO_x ranged from 4 to 21 g km⁻¹ depending on Euro class, which is in good agreement with reported values for HDVs and buses in the literature (Table 5). In comparison with the HBEFA 3.1 model, the measured values for EF_{NO_x} are on average lower for all the tested Euro classes but within the 95 % confidence interval for the Euro V with SCR and EEV buses. However, for some SCR-equipped buses and CNG buses higher EF_{NO_x} values were measured. One reason for some of the high values regarding SCR may be that it is critical that the exhaust temperature is high enough for the SCR to work properly.

In Fig. 8a there is a comparison of EF_{part} and EF_{NO_x}; both mass and number of particles show an anti-relationship with NO_x, which is especially true when no DPF is installed. In a

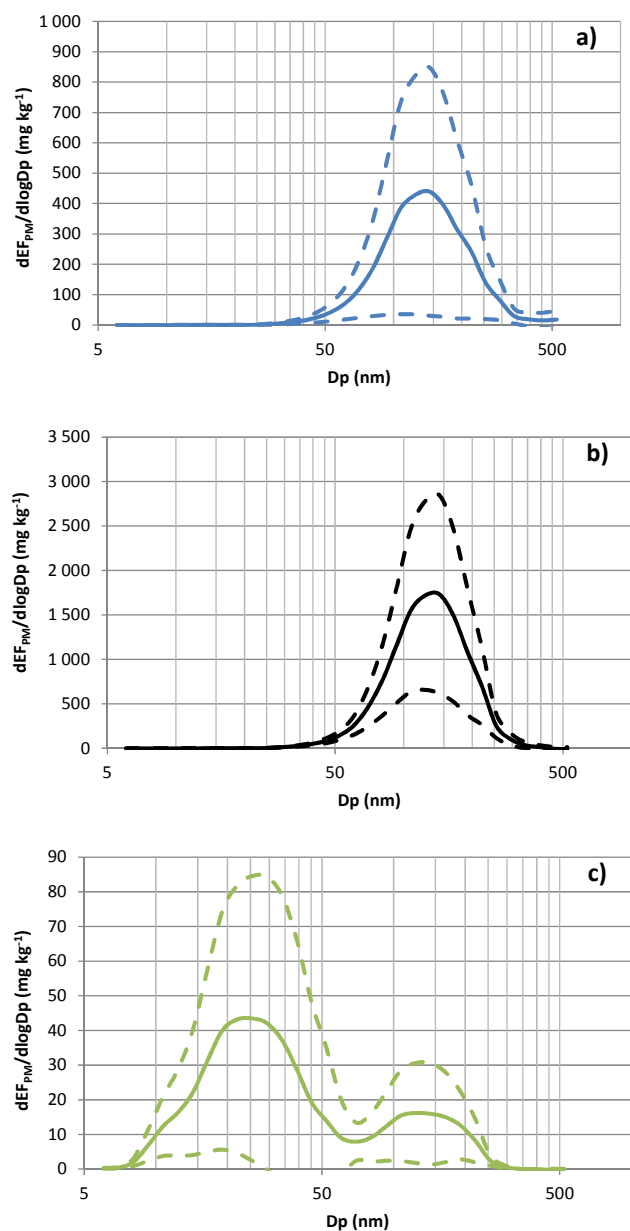


Fig. 5. Size-resolved average EF_{PM} for diesel buses (Euro III–V) with DPF (a) and without DPF (b) and for CNG buses (c) for the driving mode *acceleration*. Solid lines represent averages and dashed lines the statistical 95 % confidence interval. For the data presented in graph (b) one bus (no. 34) was excluded showing a bimodal EF_{PM} and with peak sizes of ~ 30 nm and ~ 190 nm.

diesel engine there is a compromise between emissions of NO_x and emissions of particles (Clark et al., 1999), as is demonstrated by the data in Fig. 8a. For the CNG-fuelled buses no such trend was observed.

Generally the emission of CO from a diesel engine is low as the combustion is carried out in an air-rich environment. This can be seen in the data for the tested buses, where the CO concentrations for many of the buses are below the de-

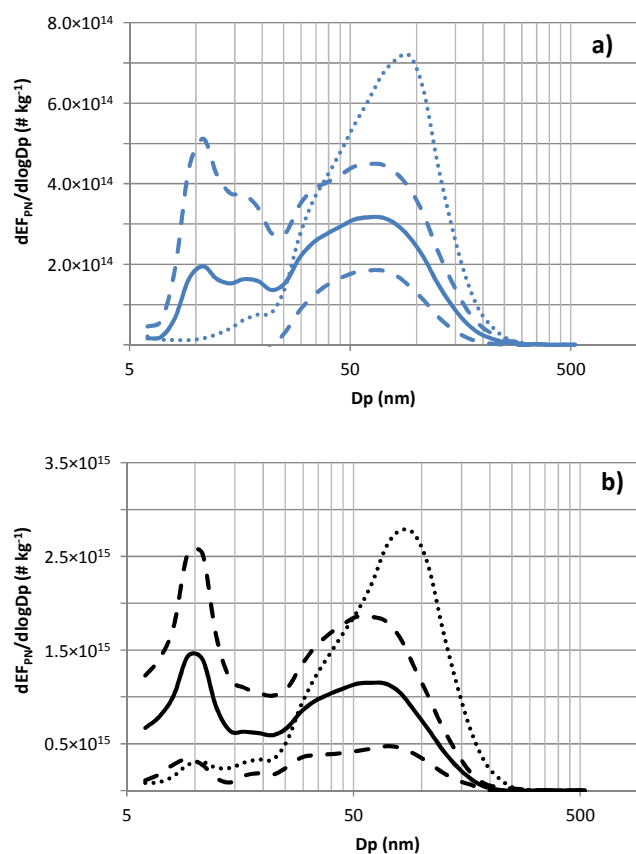


Fig. 6. Size-resolved average EF_{PN} for diesel buses (Euro III–V) with DPF (a) and without DPF (b) for the driving mode *constant speed mode*. Solid lines represent averages and dashed lines the statistical 95 % confidence interval. Dotted lines represent averages for the *accelerating mode*.

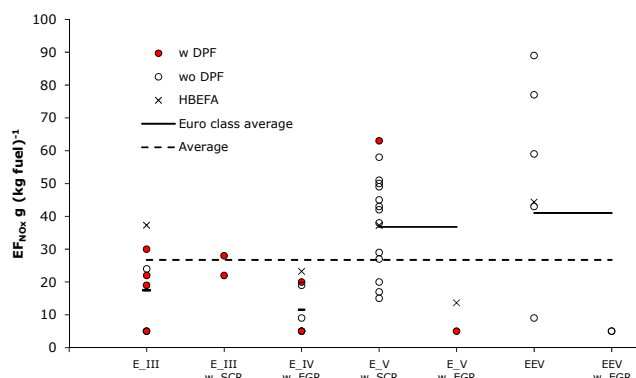


Fig. 7. EF_{NO_x} for all the buses studied divided into Euro class. Without DPF (white circles), with DPF (red circles), average of all represented Euro classes (dashed line), average of an individual represented Euro class (solid line). Crosses are EFs obtained by the HBEFA 3.1 model.

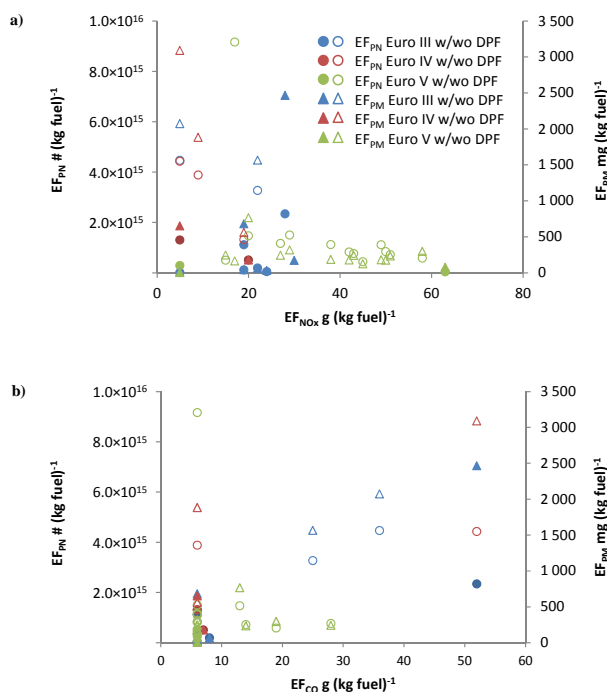


Fig. 8. EF_{PN} (circles) and EF_{PM} (triangles) versus the EF for NO_x (a) and versus the EF for CO (b). Euro III (blue symbols), Euro IV (red symbols) and Euro V (green symbols). Filled symbols represent buses with DPF installed and unfilled symbols no DPF.

tection limit of the instrument (i.e. below $18 \text{ g (kg fuel)}^{-1}$). However, for six of the buses CO concentrations were measured (3 times the std of the noise). In Fig. 8b the EF_{PM} and EF_{CO} are compared, and as is shown a positive relationship between EF_{PM} and EF_{CO} was observed. High CO concentration is an indication of incomplete combustion, hence favouring soot formation, i.e. high EF_{PM} . Regarding number of particles there is also a positive relationship, however less profound (Fig. 8b) than the relationship between EF_{PM} and EF_{CO} .

The CO emissions are also influenced by DPF. The average EF_{CO} for the diesel buses with DPF tested in this study, when assigning values below 6 (1 times the std of the noise) to $6 \text{ g (kg fuel)}^{-1}$, were $11 \text{ g (kg fuel)}^{-1}$ (10 buses in total). For the buses without DPF the average EF_{CO} was $14 \text{ g (kg fuel)}^{-1}$ (18 buses in total); hence DPF is not only reducing particles but CO as well, as reported in Ayala et al. (2002) and Lanni et al. (2001). For the tested buses, DPF had no statistical significant effect on the amount of NO_x emitted, which also is in agreement with results reported by Ayala et al. (2002).

Regarding total hydrocarbon (HC), emissions above the detection limit ($14 \text{ g (kg fuel)}^{-1}$) were not found for any of the buses in this study. Compared to the literature data shown in Table 5, values above the detection limit of our instrumentation were only reported for some CNG-fuelled buses.

4 Atmospheric implications and conclusions

The method of using a high time resolution particle instrument and CO_2 concentration as a tracer of the combustion source for determining EF_{PN} and EF_{PM} from individual vehicles for real-world dilution showed to be very successful regarding reproducibility, costs and number of vehicles studied. This method enabled measurements of not only particle number but also size, as well as mass.

Compressed natural gas buses are more advantageous regarding emissions of particle mass compared to diesel buses. However, in accelerating mode, generally CNG buses emit more particles by number compared to diesel-fuelled buses, and these particles are smaller ($D_p \sim 10 \text{ nm}$ compared to $\sim 80 \text{ nm}$) and presumably more volatile. The fact that CNG buses emit high number of particles in accelerating mode, e.g. at bus stops where many people may be standing waiting for buses, is an important aspect. However, the health impact of these particles versus diesel particles is still a matter of discussion.

This study shows that DPF markedly reduces emissions of particles both by mass and number as well as CO emissions also for real-world dilution. Reducing the number of soot mode particles does not cause a severe increase in nucleation mode particles as is the case for some of the tested CNG-fuelled vehicles without particle filter.

There was a large variation in NO_x emissions from the tested SCR-equipped buses. This is most likely due to differences in engine and exhaust temperature, which influence the efficiency of the SCR to reduce NO_x emissions. In particular this has implications for NO_2 population exposure in urban areas and is thus a health issue that needs to be investigated further.

Compared to other types of vehicles, the average EF_{PN} for a diesel-fuelled bus without DPF is very similar to results obtained for a diesel passenger car without DPF (Hak et al., 2009) when looking at the number of particles emitted per kg fuel used ($2.1 \pm 1.0 \times 10^{15} \text{ kg}^{-1}$ vs. $2.1 \pm 0.3 \times 10^{15} \text{ kg}^{-1}$). The mean EF_{PN} for DPF-equipped diesel-fuelled buses were in the same order as an old petrol car ($4.4 \pm 3.5 \times 10^{14} \text{ kg}^{-1}$ vs. $4.2 \pm 3.0 \times 10^{14} \text{ kg}^{-1}$) (Hak et al., 2009). However, when taking fuel consumption into consideration, there was a large difference. Diesel-fuelled buses without DPF are then emitting more particles per km^{-1} than a diesel passenger car without DPF, whereas DPF-equipped diesel buses are similar to a diesel passenger car without DPF ($6.5 \pm 3.2 \times 10^{14}$ and $1.4 \pm 1.1 \times 10^{14} \text{ km}^{-1}$ vs. $1.2 \pm 0.2 \times 10^{14} \text{ km}^{-1}$). On average the CNG-fuelled bus investigated in this study emitted a higher number of particles than a diesel passenger car both with respect to kg fuel burnt and per km driven.

In the data the typical trade-off trend between emission of NO_x and particles (PN and PM) was observed, especially for vehicles without DPF, as well as a positive relationship between emissions of CO and PM/PN.

The data presented in this study demonstrate the variation in gas and particle emissions of the in-use fleet of a regional public bus service, where variations found between similar buses can be due to engine specifics, maintenance or malfunction.

Acknowledgements. This work was financed by Västtrafik, the Foundation for the Swedish Environmental Research Institute, and the Graduate School Environment and Health, the University of Gothenburg. The drivers and the personnel at the measurement sites are gratefully acknowledged for their assistance and hospitality. Donald H. Stedman and Gary Bishop of Denver University are acknowledged for valuable input regarding the RSD evaluation.

Edited by: T. Petäjä

References

- Ayala, A., Kado, N. Y., Okamoto, R. A., Holmen, B. A., Kuzmicky, P. A., Kobayashi, R., and Stiglitz, K. E.: Diesel and cng heavy-duty transit bus emissions over multiple driving schedules: Regulated pollutants and project overview, SAE Technical Paper Series, 2002-01-1722, 2002.
- Ban-Weiss, G. A., Lunden, M. M., Kirchstetter, T. W., and Harley, R. A.: Size-resolved particle number and volume emission factors for on-road gasoline and diesel motor vehicles, *J. Aerosol Sci.*, 41, 5–12, 2010.
- Beddows, D. C. S. and Harrison, R. M.: Comparison of average particle number emission factors for heavy and light duty vehicles derived from rolling chassis dynamometer and field studies, *Atmos. Environ.*, 42, 7954–7966, doi:10.1016/j.atmosenv.2008.06.021, 2008.
- Birmili, W., Alaviippola, B., Hinneburg, D., Knoth, O., Tuch, T., Borken-Kleefeld, J., and Schacht, A.: Dispersion of traffic-related exhaust particles near the Berlin urban motorway – estimation of fleet emission factors, *Atmos. Chem. Phys.*, 9, 2355–2374, doi:10.5194/acp-9-2355-2009, 2009.
- Burgard, D. A., Bishop, G. A., Stadtmuller, R. S., Dalton, T. R., and Stedman, D. H.: Spectroscopy applied to mobile source emissions, *Appl. Spectrosc.*, 60, 135A–148A, 2006.
- Canagaratna, M. R., Jayne, J. T., Ghertner, D. A., Herndon, S., Shi, Q., Jimenez, J. L., Silva, P. J., Williams, P., Lanni, T., Drewnick, F., Demerjian, K. L., Kolb, C. E., and Worsnop, D. R.: Chase studies of particulate emissions from in-use new york city vehicles, *Aerosol Sci. Technol.*, 38, 555–573, 2004.
- Chen, C. H., Huang, C., Jing, Q. G., Wang, H. K., Pan, H. S., Li, L., Zhao, J., Dai, Y., Huang, H. Y., Schipper, L., and Streets, D. G.: On-road emission characteristics of heavy-duty diesel vehicles in shanghai, *Atmos. Environ.*, 41, 5334–5344, doi:10.1016/j.atmosenv.2007.02.037, 2007.
- Clark, N. N., Gautam, M., Rapp, B. L., Lyons, D. W., Graboski, M. S., McCormick, L., Alleman, T. L., and Norton, P.: Diesel and cng transit bus emissions characterization by two chassis dynamometer laboratories: Results and issues, *Soc. Autom. Eng.*, 1999-01-1469, 1999.
- Corsmeier, U., Imhof, D., Kohler, M., Kuhlwein, J., Kurtenbach, R., Petrea, M., Rosenbohm, E., Vogel, B., and Vogt, U.: Comparison of measured and model-calculated real-world traffic emissions, *Atmos. Environ.*, 39, 5760–5775, doi:10.1016/j.atmosenv.2005.06.048, 2005.
- Delfino, R. J., Sioutas, C., and Malik, S.: Potential role of ultra-fine particles in associations between airborne particle mass and cardiovascular health, *Environ. Health Perspect.*, 113, 934–946, doi:10.1289/ehp.7938, 2005.
- Donaldson, K. Li, X. Y., and MacNee, W.: Ultrafine (nanometre) particle mediated lung injury, *J. Aerosol Sci.*, 29, 553–560, 1998.
- Ekström, M., Sjödin, Å., and Adréasson, K.: On-road optical remote sensing measurements of in-use bus emissions, 14th International Symposium Transport and Air Pollution, Graz, Austria, 2005.
- Hak, C. S., Hallquist, M., Ljungström, E., Svane, M., and Pettersson, J. B. C.: A new approach to in-situ determination of roadside particle emission factors of individual vehicles under conventional driving conditions, *Atmos. Environ.*, 43, 2481–2488, doi:10.1016/j.atmosenv.2009.01.041, 2009.
- Hallquist, M., Wenger, J. C., Baltensperger, U., Rudich, Y., Simpson, D., Claeys, M., Dommen, J., Donahue, N. M., George, C., Goldstein, A. H., Hamilton, J. F., Herrmann, H., Hoffmann, T., Iinuma, Y., Jang, M., Jenkin, M. E., Jimenez, J. L., Kiendler-Scharr, A., Maenhaut, W., McFiggans, G., Mentel, Th. F., Monod, A., Prévôt, A. S. H., Seinfeld, J. H., Surratt, J. D., Szmigielski, R., and Wildt, J.: The formation, properties and impact of secondary organic aerosol: current and emerging issues, *Atmos. Chem. Phys.*, 9, 5155–5236, doi:10.5194/acp-9-5155-2009, 2009.
- Harrison, R., Jones, M., and Collins, G.: Measurements of the physical properties of particles in the urban atmosphere, *Atmos. Environ.*, 33, 309–321, 1999.
- HBEFA3.1: available online at: www.hbefa.net (last access: 13 May 2013), 2010.
- Janhall, S. and Hallquist, M.: A novel method for determination of size-resolved, submicrometer particle traffic emission factors, *Environ. Sci. Technol.*, 39, 7609–7615, 2005.
- Janhall, S., Jonsson, Å. M., Molnar, P., Svensson, E. A., and Hallquist, M.: Size resolved traffic emission factors of submicrometer particles, *Atmos. Environ.*, 38, 4331–4340, 2004.
- Jayarathne, E. R., Morawska, L., Ristovski, Z. D., and Johnson, G. R.: The use of carbon dioxide as a tracer in the determination of particle number emissions from heavy-duty diesel vehicles, *Atmos. Environ.*, 39, 6812–6821, 2005.
- Jayarathne, E. R., He, C., Ristovski, Z. D., Morawska, L., and Johnson, G. R.: A comparative investigation of ultrafine particle number and mass emissions from a fleet of on-road diesel and cng buses, *Environ. Sci. Technol.*, 42, 6736–6742, 2008.
- Jayarathne, E. R., Ristovski, Z. D., and Morawska, L.: Particle and gaseous emissions from compressed natural gas and ultralow sulphur diesel-fuelled buses at four steady engine loads, *Sci. Total Environ.*, 407, 2845–2852, 2009.
- Jayarathne, E. R., Meyer, N. K., Ristovski, Z. D., Morawska, L., and Miljevic, B.: Critical analysis of high particle number emissions from accelerating compressed natural gas buses, *Environ. Sci. Technol.*, 44, 3724–3731, doi:10.1021/es1003186, 2010.
- Jayarathne, E. R., Meyer, N. K., Ristovski, Z. D., and Morawska, L.: Volatile properties of particles emitted by compressed natural gas and diesel buses during steady-state and transient driving modes, *Environ. Sci. Technol.*, 46, 196–203, 2012.

- Jones, A. M. and Harrison, R. M.: Estimation of the emission factors of particle number and mass fractions from traffic at a site where mean vehicle speeds vary over short distances, *Atmos. Environ.*, 40, 7125–7137, doi:10.1016/j.atmosenv.2006.06.030, 2006.
- Keogh, D. U., Kelly, J., Mengersen, K., Jayaratne, R., Ferreira, L., and Morawska, L.: Derivation of motor vehicle tailpipe particle emission factors suitable for modelling urban fleet emissions and air quality assessments, *Environ. Sci. Poll. Res.*, 17, 724–739, doi:10.1007/s11356-009-0210-9, 2010.
- Kristensson, A., Johansson, C., Westerholm, R., Swietlicki, E., Gidhagen, L., Wideqvist, U., and Vesely, V.: Real-world traffic emission factors of gases and particles measured in a road tunnel in stockholm, sweden, *Atmos. Environ.*, 38, 657–673, doi:10.1016/j.atmosenv.2003.10.030, 2004.
- Kumar, P., Robins, A., Vardoulakis, S., and Britter, R.: A review of the characteristics of nanoparticles in the urban atmosphere and the prospects for developing regulatory controls, *Atmos. Environ.*, 44, 5035–5052, 2010.
- Lanni, T., Frank, B. P., Tang, S., Rosenblatt, D., and Lowell, D.: Performance and emissions evaluation of compressed natural gas and clean diesel buses at new york city's metropolitan transit authority, SAE Technical Paper Series, 2003-01-0300, 2003.
- Lopez, J. M., Jimenez, F., Aparicio, F., and Flores, N.: On-road emissions from urban buses with scr+urea and egr+dpf systems using diesel and biodiesel, *Transport. Res. Part D*, 14, 1–5, 2009.
- Maricq, M. M.: Chemical characterization of particulate emissions from diesel engines: A review, *J. Aerosol Sci.*, 38, 1079–1118, 2007.
- Morawska, L., Ristovski, Z., Jayaratne, E. R., Keogh, D. U., and Ling, X.: Ambient nano and ultrafine particles from motor vehicle emissions: Characteristics, ambient processing and implications on human exposure, *Atmos. Environ.*, 42, 8113–8138, doi:10.1016/j.atmosenv.2008.07.050, 2008.
- Norman, A. A., Kado, Y., Okamoto, R. A., Holmen, B. A., Kuzmicky, P. A., Kobayashi, R., and Stiglitz, K. E.: Diesel and cng heavy-duty transit bus emissions over multiple driving schedules: Regulated pollutants and project overview, SAE Technical Paper Series, 2002-01-1722, 2002.
- Nylund, N., Erkkilä, K., Lappi, M., and Ikonen, M.: Transit bus emission study: Comparison of emissions from diesel and natural gas buses, Research report PRO3/P5150/04, 2004.
- Pirjola, L., Parviainen, H., Hussein, T., Valli, A., Hämeri, K., Aalto, P., Virtanen, A., Keskinen, J., Pakkanen, T. A., Mäkelä, T., and Hillamo, R. E.: "sniffer"-a novel tool for chasing vehicles and measuring traffic pollutants, *Atmos. Environ.*, 38, 3625–3635, 2004.
- Pope, C. A. and Dockery, D. W.: Health effects of fine particulate air pollution: Lines that connect, *J. Air Waste Manage. Assoc.*, 56, 709–742, 2006.
- Robinson, A. L., Donahue, N. M., Shrivastava, M. K., Weitkamp, E. A., Sage, A. M., Grieshop, A. P., Lane, T. E., Pierce, J. R., and Pandis, S. N.: Rethinking organic aerosols: Semivolatile emissions and photochemical aging, *Science*, 315, 1259–1262, 2007.
- Seinfeld, J. H. and Pandis, S. N.: Atmospheric chemistry and physics: From air pollution to climate change, Wiley-Interscience, 1998.
- Shi, J. P., Harrison, R. M., Evans, D. E., Alam, A., Barnes, C., and Carter, G.: A method for measuring particle numbers from vehicles driving on the road, *Environ. Technol.*, 23, 1–14, 2002.
- Shorter, J. H., Herndon, S., Zahniser, M. S., Nelson, D. D., Wormhoudt, J., Demerjian, K. L., and Kolb, C.: Real-time measurements of nitrogen oxide emissions from in-use new york city transit buses using a chase vehicle, *Environ. Sci. Technol.*, 39, 7991–8000, 2005.
- Singer, B. C., Harley, R. A., Littlejohn, D., Ho, J., and Vo, T.: Scaling of infrared remote sensor hydrocarbon measurements for motor vehicle emission inventory calculations, *Environ. Sci. Technol.*, 32, 3241–3241, 1998.
- Stephens, R. D., Mulawa, P. A., Giles, M. T., Kennedy, K. G., Groblicki, P. J., Cadle, S. H., and Knapp, K. T.: An experimental evaluation of remote sensing-based hydrocarbon measurements: A comparison to fid measurements, *J. Air Waste Manage. Assoc.*, 46, 148–158, 1996.
- Swedish Environmental Protection Agency, available online at: www.naturvardsverket.se (last access: 13 May 2013), 2013.
- Ullman, T. L., Smith, L. R., Anthony, J. W., Slodowske, W. J., Trestrail, B., Cook, A. L., Bunn, W. B., Lapin, C. A., Wright, K. J., and Clark, C. R.: Comparison of exhaust emissions, including toxic air contaminants, from school buses in compressed natural gas, low emitting diesel, and conventional diesel engine configurations, SAE Technical Paper Series, 2003-01-1381, 2003.
- Valavanidis, A., Fiotakis, K., and Vlachogianni, T.: Airborne particulate matter and human health: Toxicological assessment and importance of size and composition of particles for oxidative damage and carcinogenic mechanisms, *J. Environ. Sci. Health Pt. C-Environ. Carcinog. Ecotoxicol. Rev.*, 26, 339–362, doi:10.1080/10590500802494538, 2008.
- Vogt, R., Scheer, V., Casati, R., and Benter, T.: On-road measurement of particle emission in the exhaust plume of a diesel passenger car, *Environ. Sci. Technol.*, 37, 4070–4076, 2003.
- Wang, F., Ketzler, M., Ellermann, T., Wählin, P., Jensen, S. S., Fang, D., and Massling, A.: Particle number, particle mass and NO_x emission factors at a highway and an urban street in Copenhagen, *Atmos. Chem. Phys.*, 10, 2745–2764, doi:10.5194/acp-10-2745-2010, 2010.
- Wang, H. K., Chen, C. H., Huang, C., and Fu, L. X.: On-road vehicle emission inventory and its uncertainty analysis for shanghai, china, *Sci. Total Environ.*, 398, 60–67, doi:10.1016/j.scitotenv.2008.01.038, 2008.
- Wang, W. G., Clark, N. N., Lyons, D. W., Yang, R. M., Gautam, M., Bata, R. M., and Loth, J. L.: Emissions comparisons from alternative fuel buses and diesel buses with a chassis dynamometer testing facility, *Environ. Sci. Technol.*, 31, 3132–3137, 1997.